# Cryo-TEMPO

## Algorithm Theoretical Basis Document

## Sea Ice


| | | | |
|---|---|---|---|
| Prepared by | : | S. Hendricks | 22/6/2022 |
| Checked by | : | M. McMillan | 21/7/2022 |
| Approved by | : | | |

# Change Log

| Issue | Author | Affected Section | Change | Status |
|---|---|---|---|---|
| 0 | Stefan Hendricks, AWI | All | Document Creation | Complete |
| 1.1 | Stefan Hendricks, AWI | All | Version 1 Content | Complete |
| 1.2 | Stefan Hendricks, AWI | All | Version 1 Revisions | Complete |
| 2.1 | Stefan Hendricks, AWI | All | Algorithm Update (Phase 2.1) | In Review |

# Acronyms and Abbreviations

| | | | |
|---|---|---|---|
| AD | Applicable Document | REAPER | REprocessing of Altimeter Products for ERs |
| ADT | Absolute Dynamic Topography | RFW | Request for Waiver |
| ATM | Airborne Topographic Mapper | RMSD | Root mean square difference |
| AWI | Alfred Wegener Institute | SAR | Synthetic Aperture Radar |
| C3S | Copernicus Climate Change Service | SARIn | Synthetic Aperture Radar Interferometric |
| CCI | Climate Change Initiative | SL | Science Lead |
| CCN | Contract Change Notice | SLA | Sea Level Anomaly |
| CLS | Collecte Localisation Satellites | SIGMA0 | Sigma Nought |
| CNES | Centre National des Etudes Spatiales (French Space Agency) | SoW | Statement of Work |
| CNR | Consiglio Nazionale delle Ricerche | SS | Shepherd Space |
| CPOM | Centre for Polar Observation & Modelling | TCOG | Threshold Centre of Gravity |
| CR | Change Request | TDP | Thematic Data Product |
| CRISTAL | Copernicus Polar Ice and Snow Topography Altimeter | TFMRA | Threshold First Maximum Retracker Algorithm |
| CryoVEx | Cryosat Validation Experiment (field campaigns) | TUG | Thematic User Group |
| DAHITI | Database for Hydrological Time Series of Inland Waters | UCL | University College London |
| DEM | Digital Elevation Model | UCM | User Consultation Meeting |
| DTU | Technical University of Denmark | WP | Work Package |
| EO | Earth Observation | | |
| ERR | Evolutions Recommendation Report | | |
| ESA | European Space Agency | | |
| FIS | Finnish Ice Service | | |
| FMI | Finnish Meteorological Institute | | |
| FRAPPE | Flexible Radar Altimeter Processor for Performance Evaluation | | |
| FRM4ALT | Fiducial Reference Measurement for Altimetry | | |
| FRD4ALT | Fundamental Data Records for Altimetry | | |
| FYI | First-year sea ice | | |
| G-REALM | Global Reservoirs and Lakes Monitor | | |
| IMEDEA | Instituto Mediterráneo de Estudios Avanzados | | |
| IPCC | Intergovernmental Panel on Climate Change | | |
| IRPI | Istituto di Ricerca per la Protezione Idrogeologica | | |
| ISRO | Indian Space Research Organisation | | |
| ITT | Invitation To Tender | | |
| JPL | Jet Propulsion Laboratory | | |
| LEGOS | Laboratoire d'Étude en Géophysique et Océanographie Spatiale | | |
| LEW | Leading Edge Width | | |
| LRM | Low Resolution Mode | | |
| LU | Lancaster University | | |
| MDT | Mean Dynamic Typography | | |
| MSS | Mean Sea Surface | | |
| MSSL | Mullard Space Science Laboratory (part of UCL) | | |
| MYI | Multi-year sea ice | | |
| NCR | Non Conformance Report | | |
| NERSC | Nansen Environmental and Remote Sensing Center | | |
| NSIDC | National Snow and Ice Data Center | | |
| OCOG | Offset Centre Of Gravity retracker | | |
| PDS | Payload Data Segment | | |
| PEG | Polar Expert Group | | |
| PM | Project Manager | | |
| PO | Polar Oceans | | |
| PP | Pulse Peakiness | | |
| PSMSL | Permanent Service for Mean Sea Level | | |
| RA | Radar Altimeter / Altimetry | | |

# Table of Contents

# 1 INTRODUCTION

## 1.1 Purpose and Scope

This document comprises the Algorithm Theoretical Basis (ATBD) for the sea ice algorithm used for the *CryoSat-2 ThEMatic PrOducts* (*Cryo-TEMPO*) study, Ref: ESA AO/1-10244/2-/I-NS. The ATBD has been written by the sea ice team led by the Alfred Wegener Institute, with contributions from all members of the Cryo-TEMPO consortium. Lancaster University as the prime contractor is the contact point for all communications regarding this document.

The Algorithm Theoretical Basis Document (ATBD) provides a high-level description of the algorithms and processing used to produce each Cryo-TEMPO sea ice product parameter.

## 1.2 Document Structure

This document describes the algorithms of the sea ice processing chain. The document is structured as follows:

- **Section 1 – Introduction**
- **Section 2 – Sea Ice Parameters**
- **Section 3 – Overall Sea Ice Processing Flow**
- **Section 4 – Algorithm Descriptions**
- **Section 5 – Data Examples**
- **Section 6 – Known Issues**

## 1.3 Applicable and Reference Documents

### Applicable documents

| Reference | Title |
|---|---|
| **AD1** | Statement of Work ESA Express Procurement Plus - EXPRO+ CryoSat-2 ThEMatic PrOducts \| Cryo-TEMPO, Issue 1, Revision 0, Date of Issue 01/04/2020 [Ref. ESA-EOPG-EOPGMQ-SOW-10]. |
| **AD2** | Invitation to Tender for CryoSat-2 ThEMatic PrOducts \| Cryo-TEMPO REF.: ESA AO/1-10244/2-/I-NS [Ref. SA-IPL-POE-NS-sp-LE-2020-313]. |
| **AD3** | Draft Contract, CryoSat-2 ThEMatic PrOducts \| Cryo-TEMPO, Appendix 2 to ESA AO/1-10244/20/I-NS. |

### Reference documents

| Reference | Title |
|---|---|
| **RD1** | Copernicus Polar and Snow Cover Applications User Requirements Workshop, http://www.copernicus.eu/polar-snow-workshop |
| **RD2** | PEG-1 Report, User Requirements for a Copernicus Polar Mission, Step 1 Report, Polar Expert Group, Issue: 12th June 2017 |
| **RD3** | PEG-2 Report, Polar Expert Group, Phase 2 Report on Users Requirements, Issue: 31st July 2017 |

# 2 SEA ICE PARAMETER

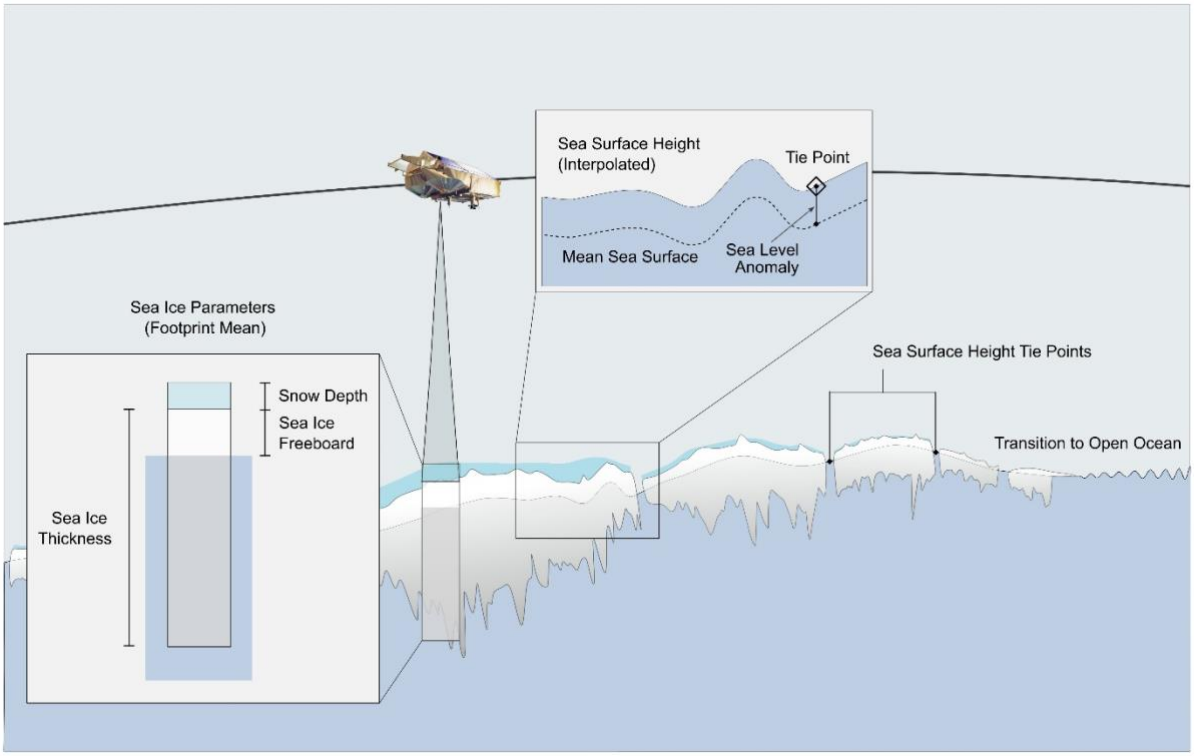


**Figure 1: Schematic of sea-ice freeboard and snow depth retrieval from CryoSat-2 altimeter track data**

## 2.1 Parameter Definition

The Cryo-TEMPO thematic sea ice product contains geolocated and time-associated sea-ice freeboard, the elevation of the ice surface above local sea level as well as snow depth on sea ice. Both variables are fundamental input parameters for the estimation of sea-ice thickness. Sea ice thickness and snow depth have also recently been acknowledged asEssential Climate Variables (ECV)(Lavergne et al., 2022). A full definition of the two parameters as well as their standardized names are given in Table 1.

The product files contain information at the full resolution of CryoSat's radar altimeter SIRAL since the geophysical retrieval is based on input data of individual orbits in the polar regions. The geophysical output maintains the location and time of each radar waveform in the CryoSat-2 Level-1b sensor data along the trajectory and thus fulfils the requirements for level 2 data processing.

Sea ice freeboard is the geophysical parameter that is directly derived from observations by the radar altimeter, except for a range correction over ice surfaces that depends on external snow depth information. Freeboard is expected to show variability at scales significantly smaller than the size of the CryoSat-2 footprint, thus the presented values in the product files indicate the mean sea-ice

freeboard within the CryoSat-2 footprint. Significant variability between adjacent observations is also expected due to true variability as well as sensor noise and potential retrieval biases.

Snow depth on sea ice instead is not measured by the CryoSat-2 radar altimeter and the information in the Cryo-TEMPO thematic sea ice product originate from lower resolution auxiliary data sources. Snow depth data is nevertheless provided at full spatial resolution as it is an input parameter for the per-waveform sea-ice freeboard retrieval. Like sea-ice freeboard, the snow depth values are expected to represent the mean snow depth in the CryoSat-2 footprint.

**Table 1: Definition of geophysical sea ice variables and their names in the Cryo-TEMPO thematic sea ice product. Standard names and the definition are taken and modified from the table of standard names for the Climate and Forecast (CF) metadata conventions for earth science datasets.**

| **Parameter** | **Property** | |
|---|---|---|
| Sea Ice Freeboard | *Variable Name* | sea_ice_freeboard |
| | *Unit* | meter (m) |
| | *CF Standard Name* | sea_ice_freeboard |
| | *Definition* | Sea ice freeboard is the mean height of the sea-ice surface above the water surface in the horizontal domain. "Sea ice" means all ice floating in the sea which has formed from freezing sea water, rather than by other processes such as calving of land ice to form icebergs. |
| Sea Ice Freeboard Uncertainty | *Variable Name* | sea_ice_freeboard_uncertainty |
| | *Unit* | meter (m) |
| | *CF Standard Name* | sea_ice_freeboard standard_error |
| | *Definition* | The retrieval uncertainty of sea-ice freeboard |
| Filtered Sea Ice Freeboard | *Variable Name* | sea_ice_freeboard_filtered |
| | *Unit* | meter (m) |
| | *CF Standard Name* | sea_ice_freeboard |
| | *Definition* | A smoothed representation of sea_ice_freeboard with an along-track lowess filter. |
| Radar Freeboard | *Variable Name* | radar_freeboard |
| | *Unit* | meter (m) |
| | *CF Standard Name* | - |
| | *Definition* | Freeboard measurement of the radar altimeter. Does not contain a range offset correcting for a signal delay caused by the radar wave propagation through the snow layer. |
| Radar Freeboard Uncertainty | *Variable Name* | radar_freeboard_uncertainty |
| | *Unit* | meter (m) |
| | *CF Standard Name* | - |
| | *Definition* | The retrieval uncertainty of radar freeboard |
| Snow Depth on Sea Ice | *Variable Name* | snow_depth |
| | *Unit* | meter (m) |
| | *CF Standard Name* | surface_snow_thickness |
| | *Definition* | Surface snow refers to the snow on the solid ground or on surface ice cover, but excludes, for example, falling snowflakes. "Thickness" means the vertical extent of a layer and is assumed to apply to the whole area of each horizontal domain. |
| Snow Depth Uncertainty | *Variable Name* | snow_depth_uncertainty |
| | *Unit* | meter (m) |
| | *CF Standard Name* | surface_snow_thickness standard_error |
| | *Definition* | The uncertainty of snow depth on sea ice from the source climatologies |

**Table 2: Definition of geolocation variables and their names in the Cryo-TEMPO thematic sea ice product. Standard names and the definition are taken and modified from the table of standard names for the Climate and Forecast (CF) metadata conventions for earth science datasets.**

| Parameter | Property | |
|---|---|---|
| time | *Variable Name* | time |
| | *Unit* | seconds since 2000-01-01 00:00:00 |
| | *CF Standard Name* | time |
| | *Definition* | UTC time counted in seconds since 2000-01-01 00:00:00 (Gregorian calendar) |
| Longitude | *Variable Name* | longitude |
| | *Unit* | degrees east |
| | *CF Standard Name* | longitude |
| | *Definition* | Longitude of satellite nadir measurement location [-180, 180]. Positive longitude is East relative to Greenwich meridian. |
| Latitude | *Variable Name* | latitude |
| | *Unit* | Degrees north |
| | *CF Standard Name* | latitude |
| | *Definition* | Latitude of satellite nadir measurement location [-90, +90]. Positive latitude is North latitude, negative latitude is South latitude. |

## 2.2 Target Audience and Intended Use

The target audience for Cryo-TEMPO thematic sea ice product are users of sea ice remote sensing data who require access for low level geophysical parameters with the full resolution and a minimum of applied processing steps and assumptions made therein.

Potential use cases are for example:

1. Evaluation of custom sea-ice freeboard algorithms
2. Implementation of custom sea-ice freeboard to sea-ice thickness conversion processing chains.
3. Using sea-ice freeboard data for customized grids or aggregated time periods
4. Using sea-ice freeboard as an analogue to an observation operator as low-level comparison between satellite remote sensing and numerical sea-ice simulations.

While sea-ice thickness is a required parameter for many end-users in climate research and operational sea-ice remote sensing applications, it is not included in the Cryo-TEMPO thematic sea ice product due to the scope of a low-level sea-ice remote sensing data set. However, user feedback is welcome, and the content of the thematic sea ice product may be extended in future versions.

## 2.3 Geographical Coverage

The Cryo-TEMPO thematic sea ice product covers the northern hemisphere, which is defined here as all CryoSat-2 SAR and SARin data over sea-ice covered regions north of 45N (see Figure 2). Data in the southern hemisphere will be added in future versions.

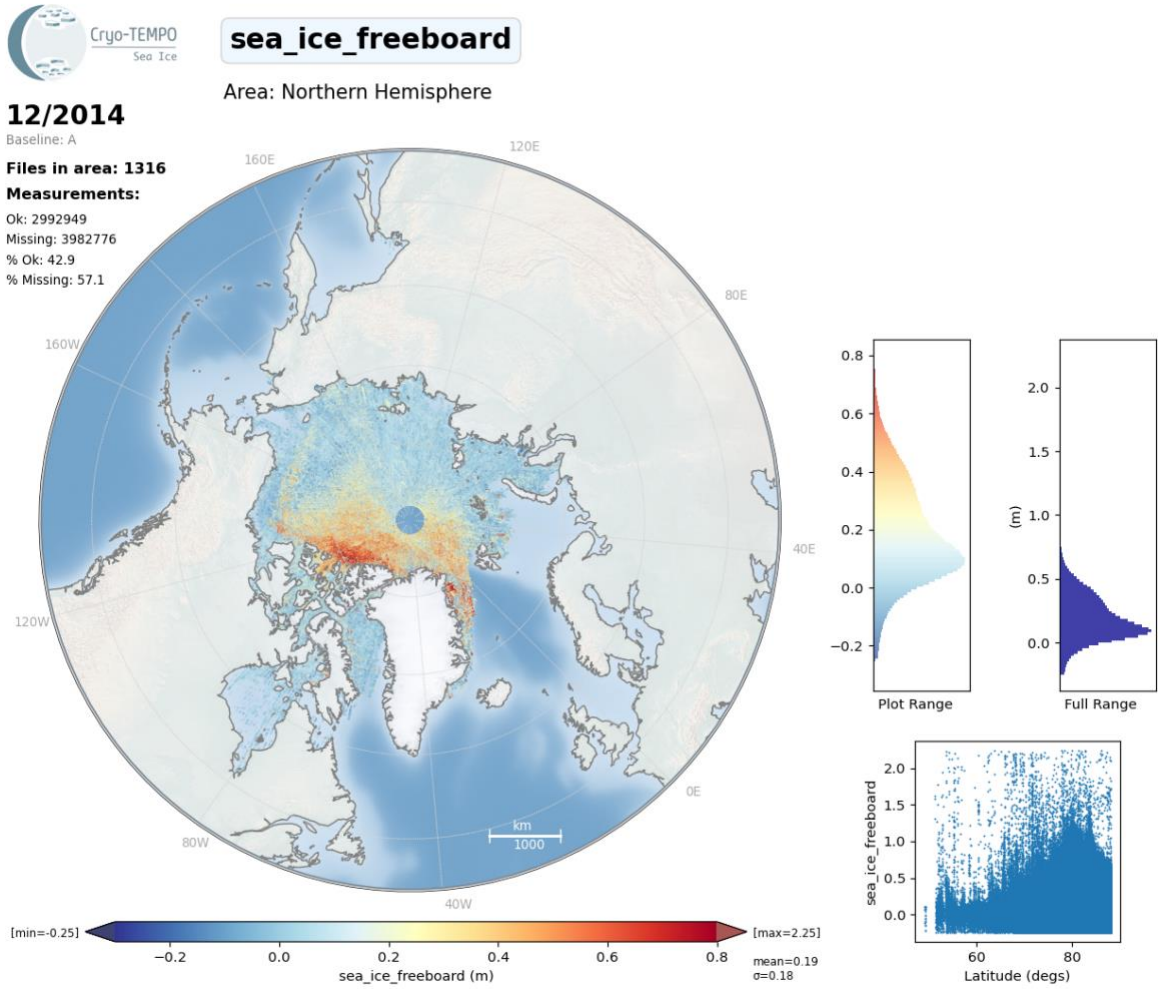


**Figure 2: Geographical coverage of the Cryo-TEMPO thematic sea ice product.**

# 3 OVERALL SEA ICE PROCESSING FLOW

The fundamental principle of sea-ice freeboard retrieval is based on measuring the elevations of sea ice surfaces and the local sea level at fractures in the ice cover. Sea ice freeboard is then computed by taking the difference between the sea ice elevations, corrected to account for propagation through the snow layer, and an interpolated sea level along the satellite track (see Figure 1). The processing is applied to each polar orbit individually.

This geophysical processing chain is broken down into several distinct sub-steps (

Figure 3):

1. Surface type classification of each waveform into categories of open ocean, lead (water or very thin ice at fractures of the sea ice covers, sea ice and ambiguous. (See Section 4.3.2)
2. Estimation of radar range (retracking) between the satellite and the surface for each waveform of the surface types lead and sea ice.
3. Computation of surface elevation by subtracting radar range from the altitude of the satellite.
4. Application of range corrections to the elevation profile to account for signal delay effects caused by varying radar wave propagation speed in the iono- and troposphere.
5. Removal of the effect of tides on the along-track elevations
6. Removal of static sea surface height variations by subtracting a mean sea surface height from the along-track elevations.
7. Along-track interpolation of the sea-level anomaly from the discrete observations (lead elevations) of sea surface height in the ice cover
8. Range correction over snow covered sea ice due to the lower wave propagation speed inside the snow layer.

The estimation of the along-track sea-level anomaly is shared with the polar ocean thematic product and implemented in a consistent way. There are two main assumptions in the processing:

1. All parameter values represent the mean value in the radar altimeter footprint.
2. The main reflecting horizon for Ku-Band altimeter data in the Arctic winter season is the snow/ice interface.

The limitations of these assumptions are discussed in section 6.

The overall processing flow depend on the primary radar altimeter data as well as several auxiliary data sets that are required for accurate retrieval of sea-surface height and sea-ice freeboard:

1. Sea Ice Concentration data is used as a daily sea-ice mask aiding the surface type classification.

2. A static mean sea surface describes the average variation of the ocean surface. Removing this variation from the along-track elevations reduces the probability of interpolation errors between distant instantaneous sea-surface height observations at the location of leads.
3. A Snow climatology describes the average monthly evolution of snow depth on sea ice. Snow depth and density information is required to apply a range correction caused by the specific radar wave propagation speed in the snow layer in sea-ice freeboard retrieval process.
4. Sea ice type data is used as input to the estimation of snow depth in the central Arctic Basin. This step is required because the snow depth climatology must be applied with separate value for first-year (FYI) and multi-year (MYI) sea ice and the region and temporal distribution of the two sea ice classifications is provided by an external daily gridded sea-ice type data set.

The specifications of the primary and auxiliary data sets are described in 4.1.

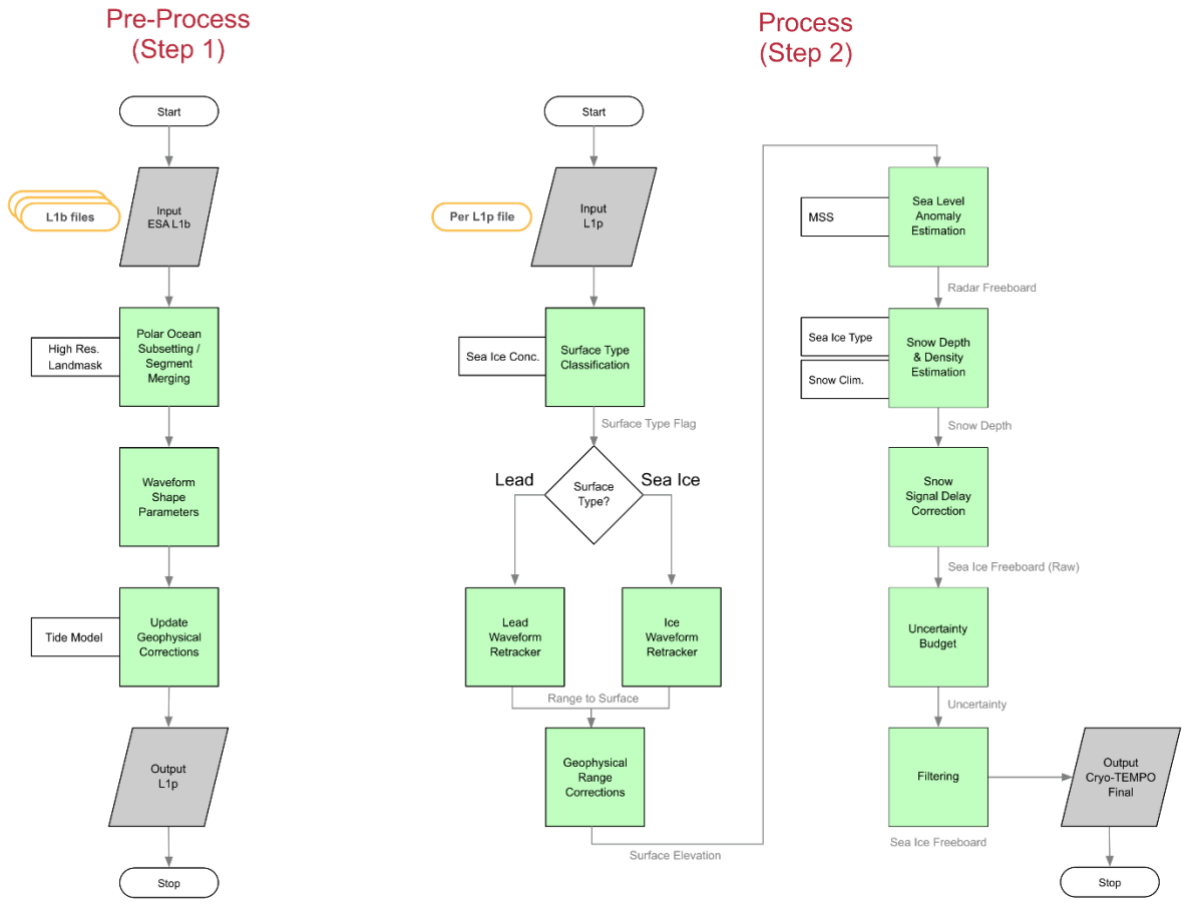


**Figure 3: Processing workflow of geophysical retrieval of sea-ice freeboard and snow depth on sea ice for the Cryo-TEMPO sea ice product.**

# 4 ALGORITHM DESCRIPTION

## 4.1 Source Data

Input data to the sea ice processing algorithm falls into two categories:

1. Primary data: Radar altimeter data from the CryoSat's SIRAL.
2. Auxiliary data: External data sets aiding the calibration or geophysical retrieval.

Each data set is described in corresponding sections below.

### 4.1.1 CryoSat-2 altimeter data

Primary input data to the Cryo-TEMPO thematic sea ice product is Level-1b data from the ESA CryoSat-2 baseline-D ICE processing chain for SAR and SARin radar modes. The files are delivered as one netCDF file separated by changes of the radar mode. Information about the CryoSat-2 products of the ICE processor can be found here:

https://earth.esa.int/web/guest/missions/cryosat/ipf-baseline

The following variables are used from the baseline-D Level-1b netCDF files:

**Table 3: List of variables from the CryoSat-2 level-1b primary input data for the sea ice processing chain**

| | |
|---|---|
| **Time-orbit data** | |
| time_20_ku | Data record time in TAI |
| lon_20_ku | Longitude of measurement |
| lat_20_ku | Latitude of measurement |
| alt_20_ku | Altitude of CoG above reference ellipsoid |
| **SIRAL waveform data** | |
| pwr_waveform_20_ku | Normalized echo power waveform |
| echo_scale_factor_20_ku | Echo Scale Factor (to scale echo to watts) |
| echo_scale_pwr_20_ku | Echo Scale Power (a power of 2) |
| window_del_20_ku | Window Delay (2way) corrected for instrument delays |
| **Instrument Flags** | |
| flag_mcd_20_ku | Level 1b Measurement Confidence Data |
| **Surface Type Flag** | |
| surf_type_01 | Surface type flag (1Hz, interpolated to time_20_ku) |
| **Range Corrections** | |
| mod_dry_tropo_cor_01 | Dry Tropospheric Correction (1Hz, interpolated to time_20_ku) |
| mod_wet_tropo_cor_01 | Wet Tropospheric Correction (1Hz, interpolated to time_20_ku) |
| hf_fluct_total_cor_01 | Dynamic Atmosphere Correction (1Hz, interpolated to time_20_ku) |
| iono_cor_01 | Ionosphere Correction (1Hz, interpolated to time_20_ku) |
| solid_earth_tide_01 | Solid Earth Tide Correction (1Hz, interpolated to time_20_ku) |
| pole_tide_01 | Geocentric Pole Tide Correction (1Hz, interpolated to time_20_ku) |

### 4.1.2 Auxiliary Data

Auxiliary data sets are data sets that are input to the geophysical retrieval but are not a measurement of the CryoSat-2 radar altimeter. Auxiliary data sets can be static fields or data sets from satellite observations with variable temporal coverage and resolution.

#### 4.1.2.1 Sea Ice Concentration

Daily sea-ice concentration fields at a spatial resolution of 25km is used as a sea ice mask in the sea-ice freeboard retrieval. The data source is the Global Sea Ice Concentration Climate Data Record produced by the European Organisation for the Exploitation of Meteorological Satellites (EUMETSAT) Ocean and Sea Ice Satellite Application Facility (OSI SAF).

The data is available in from a THREDDS Data Server (TDS) of MET Norway and through the Climate Data Store (CDS) of the Copernicus Climate Change Services (C3S).

| | |
|---|---|
| **Parameter** | Sea ice concentration (sea ice area fraction) |
| **Unit** | percent |
| **Data Source** | MET Norway (https://thredds.met.no/thredds/c3s/c3s.html) |
| **Data DOI** | https://doi.org/10.24381/cds.3cd8b812 |

#### 4.1.2.2 Sea Ice Classification

Daily sea ice classification fields at a spatial resolution of 25km from measurements of the Scanning Multichannel Microwave Radiometer (SMMR), Special Sensor Microwave/Imager (SSM/I), and Special Sensor Microwave Imager/Sounder (SSMIS) sensors are ingested for the estimation of snow depth on sea ice. The sea ice classification provides an ice type flag in the categories:

1. First-year sea ice (FYI)
2. Multi-year sea ice (MYI)
3. Ambiguous
4. Unclassified

The data is available in from a THREDDS Data Server (TDS) of MET Norway and through the Climate Data Store (CDS) of the Copernicus Climate Change Services (C3S) and is produced by the European Organisation for the Exploitation of Meteorological Satellites (EUMETSAT) Ocean and Sea Ice Satellite Application Facility (OSI SAF).

| | |
|---|---|
| **Parameter** | Sea ice type (sea ice classification) |
| **Unit** | flag |
| **Data Source** | MET Norway (https://thredds.met.no/thredds/c3s/c3s.html) |
| **Data DOI** | https://doi.org/10.24381/cds.29c46d83 |

#### 4.1.2.3 Mean Sea Surface Elevation

The global high resolution mean sea surface with a spatial resolution of 1 minute from DTU Space (Version DTU21) is used to facilitate the estimation of sea-level along the ground-track of CryoSat-2. This data set is static and used for the entire CryoSat-2 data record.

| | |
|---|---|
| **Parameter** | Elevation of mean surface |
| **Unit** | meter |
| **Data Source** | DTU-SPACE (https://ftp.space.dtu.dk/pub/DTU21/1_MIN/) |

#### 4.1.2.4 Climatology of Snow Depth on Sea Ice

The estimation of snow depth is partly based on a monthly snow depth climatology described in Warren et al., 1999, hereafter referred to as the W99 snow depth climatology. The climatology is available as two-dimensional quadratic fit coefficients that can be used to compute values of snow depth, density, and variability for given geographical coordinates. The domain of validity for W99 is the central Arctic basin.

#### 4.1.2.5 Passive Microwave Observations of Snow Depth on Sea Ice

Additional input to the snow depth retrieval algorithm in the sea ice processor are daily snow depth fields on Arctic sea ice from passive microwave observations from Advanced Microwave Scanning Radiometer 2 (AMSR2) produced by the Institute of Environmental Physics (IUP) of the University Bremen. Snow depth retrieval from AMRS2 data is based on the work of Markus and Cavalieri, 1998 and only valid over first-year sea ice. It must be noted that a newer version of the IUP data set is currently available (Rostosky et al., 2018), compared to the version 1.0 used for the snow depth climatology in the Cryo-TEMPO sea ice product.

#### 4.1.2.6 Arctic Regions

The 2021 version of the regional mask for Arctic sea ice trends and climatologies defines commonly used regions relevant for Arctic sea ice as polygons for each region (Scott Stewart and Walter N. Meier, NSIDC). The region definition was supplied by NSIDC in shapefile format and the id number of each region has been gridded on an EASE2 grid with a resolution of 1 km (Figure 4 and Table 4). The region id is added to each freeboard and snow depth value along the CryoSat-2 ground track to allow easy assessment of sea ice results by region.

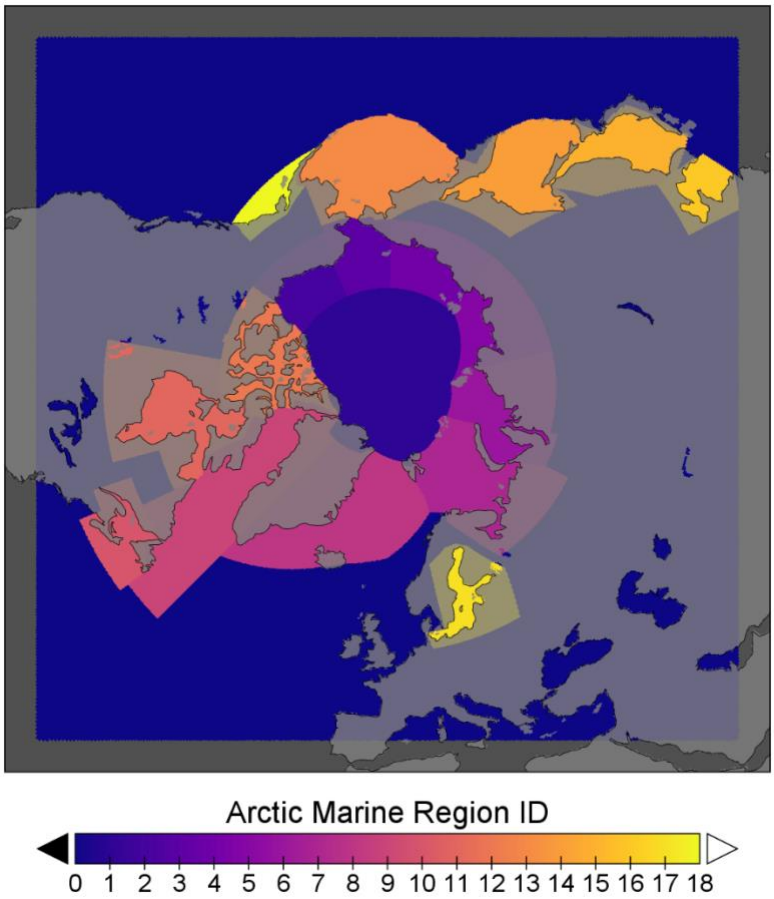


**Figure 4: Map of region id's from the 2021 version of the regional mask for Arctic sea ice trends and climatologies (credit J. Scott Stewart and Walter N. Meier, NSIDC).**

**Table 4: Region id's and their name from the 2021 version of the regional mask for Arctic sea ice trends and climatologies (credit J. Scott Stewart and Walter N. Meier, NSIDC).**

| ID | Region Name | ID | Region Name |
|---|---|---|---|
| 0 | Undefined Region | 10 | Gulf of St. Lawrence |
| 1 | Central Arctic | 11 | Hudson Bay |
| 2 | Beaufort Sea | 12 | Canadian Archipelago |
| 3 | Chukchi Sea | 13 | Bering Sea |
| 4 | East Siberian Sea | 14 | Sea of Okhotsk |
| 5 | Laptev Sea | 15 | Sea of Japan |
| 6 | Kara Sea | 16 | Bohai Sea |
| 7 | Barents Sea | 17 | Baltic Sea |
| 8 | East Greenland Sea | 18 | Gulf of Alaska |
| 9 | Baffin Bay & Labrador Sea | | |

#### 4.1.2.7 High resolution land mask

A gridded land-ocean mask for the Arctic regions at a resolution of 250 m has been created based on shapefiles of the OpenStreetMap[1] project except for the landmass of Greenland, which is sourced from the Natural Earth project[2]. The reason for the two-source solution is a better agreement of the Natural Earth shapefile with the Greenland topography from Global 30 Arc-Second Elevation (GTOPO30) digital elevation model, while the OpenStreetMap shapefiles provide more detail in the rest of the Arctic.

## 4.2 Snow Depth on Sea Ice

Snow depth on sea ice is a geophysical parameter that is not measured at the same spatial coverage and resolution of the CryoSat-2 radar altimeter data. A consistent snow depth data source for the entire CryoSat-2 data record can therefore only be obtained from a climatology or the result of numerical simulations that model snow accumulation on sea ice based on precipitation from reanalysis data.

The Cryo-TEMPO thematic sea ice product utilizes the climatology approach, based on data fusion of the W99 climatology (see section 4.1.2.4) with passive microwave data (see section 4.1.2.5) to overcome the individual limits of both data sets, namely the regional limit of the W99 sea ice climatology and the FYI limitation of the passive microwave data.

The merged climatology is computed monthly between October and April for the application to the Arctic winter season. The merged climatology is static for these months and the data is ingested as an auxiliary data file into the sea ice processor. The monthly files can be downloaded from the following ftp site:

ftp://ftp.awi.de/sea_ice/auxiliary/snow_on_sea_ice/w99_amsr2_merged/

This section provides a description of how the data sources were merged and how the data is used in the sea ice processor.

### 4.2.1 Data Fusion of Climatology and Satellite Data

To merge the two data sources, monthly composites by averaging daily IUP AMSR2 snow depth fields have been created to match the monthly resolution of the W99 climatology for October to April. A low pass filter is applied to the IUP AMSR2 snow depth composite to remove artefacts associated to specific ice conditions using a Gaussian filter with the size of 8 grid cells (50km). In additions, spurious negative snow depth values are removed, and the upper snow depth range is limited to 60 cm.

The principal objective is to use the W99 climatology in the central Arctic Basin and the filtered monthly composite in the remaining sea ice covered marine areas of the northern hemisphere. To ensure continuity between the two domains, a regional weight factor w is computed based on a

[1] https://www.openstreetmap.org/
[2] https://www.naturalearthdata.com/

regional mask based on the assumed validity of the W99 climatology. The mask consists of the central Arctic Basin with a weight factor w of 1 indicating full validity of W99 snow depth information. Outside the central Arctic Basin, the weight factor is reduced to 0 over a distance of 250 km (Figure 5).

The monthly merged snow depth climatology $sd_{merged}$ is computed as:

$$sd_{merged} = w \cdot sd_{W99} + (1 - w) \cdot sd_{AMSR2}$$

See Figure 6 for visual examples of the merging steps.

It is however common practice to modify the W99 snow climatology by reducing its value by 50% over first-year sea ice in the central Arctic. We therefore use the sea ice type auxiliary data set (section 4.1.2.2) to modify the climatology along each orbit trajectory. The sea ice type data is used in the sense of multi-year ice fraction ($f_{myi}$) with a value between 0 (100% FYI) and 1 (100% MYI). The result is the snow depth on sea ice ($sd$), or surface snow thickness, of the Cryo-TEMPO thematic sea ice product. The reduction is only applied for the W99 contribution to the merged snow depth value resulting in following approach where *c_fyi*=0.5 is the W99 scaling for first-year sea ice, c the total scaling factor that includes the multi-year sea ice fraction f_myi and the weight factor:

$$c = \left(1 - f_{myi}\right) * c_{fyi} * w$$
$$sd = sd_{merged} - c \cdot sd_{merged}$$

### 4.2.2 Uncertainty

The snow depth uncertainty is computed like the computation steps in the previous section. All input data sets provide an uncertainty value, the AMSR2 provides a spatially variable retrieval uncertainty ($\sigma_{sd}^{AMSR2}$) and the W99 climatology provides interannual variability as uncertainty ($\sigma_{sd}^{W99}$) and the sea ice type a retrieval uncertainty ($\sigma_{f_{myi}}$).

$$\sigma_{sd}^{merged} = w \cdot \sigma_{sd}^{W99} + (1 - w) \cdot \sigma_{sd}^{AMSR2}$$

$$\sigma_{sd} = \left(\sigma_{sd}^{merged} - c \cdot \sigma_{sd}^{merged}\right) + \left(sd \cdot c \cdot \sigma_{f_{myi}} \cdot c_{fyi}\right)$$

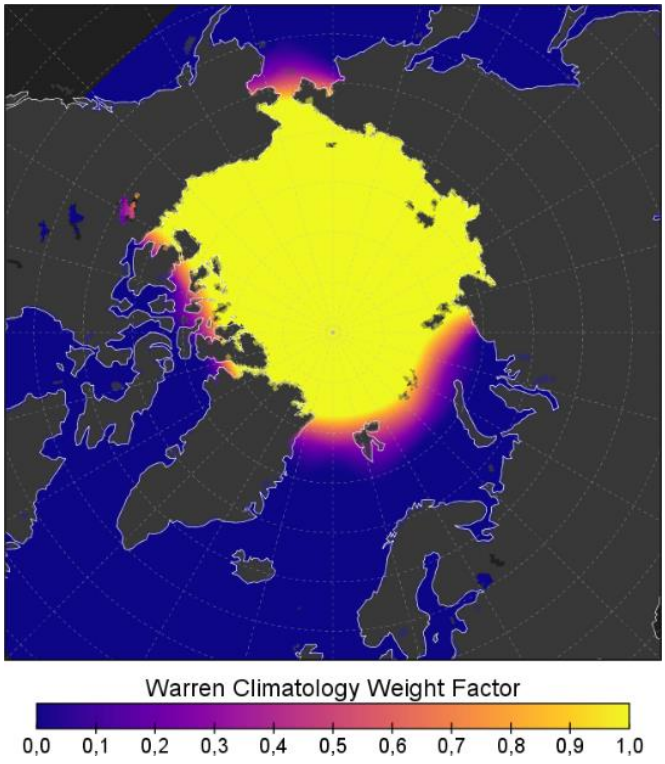


**Figure 5: Regional W99 snow climatology weight factor $w$**

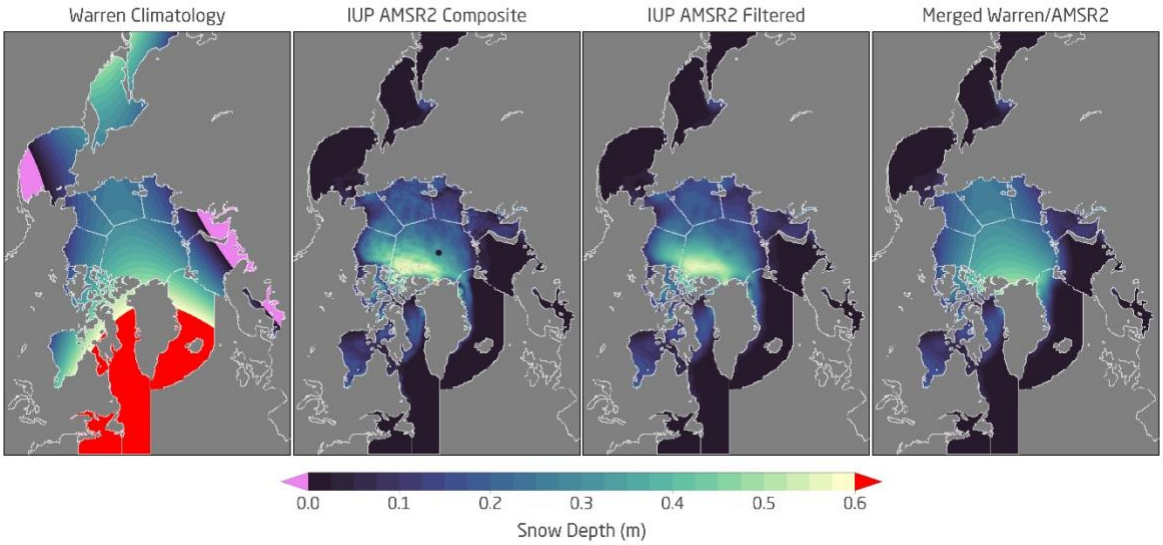


**Figure 6: Snow depth data fusion for monthly climatology based on W99 climatology and monthly averaged data from AMSr2 (IUP Bremen).**

## 4.3 Sea Ice Freeboard

This section describes the sea-ice freeboard processing chain with input from all auxiliary data and the snow depth data described in Section 4.2.

### 4.3.1 Pre-processing of Level-1b data

A regional subset of latitudes higher than 45 degrees North is used to limit the available CryoSat-2 L1b SAR and SARin data. For these two subsets, all data files of a one orbit are merged into a single orbit segment, since input data may be distributed into different files based on the radar mode. The objective is to create a continuous data segment over marine areas. Longer data segments over land are cropped from the data set (see Figure 7 for an example).

The subsetting to the Arctic Ocean domain is based on the high resolution land/ocean mask, which replaces the surface type mask included in the CryoSat-2 l1b data (variable surf_type_01).

In addition, waveform shape parameter used for surface type classification (Section 4.3.2) is computed, the timestamp is converted from TAI to UTC and the merged L1b data subset is stored in of processing level 1-preprocessed (l1p) internally on the production system.

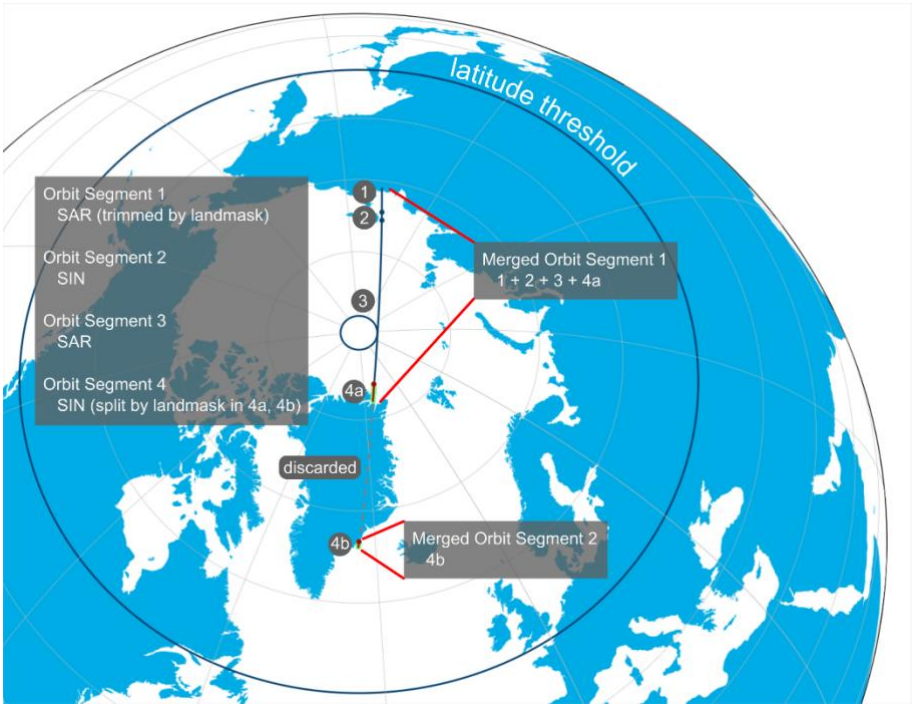


**Figure 7: Exemplary radar data selection and merging process of SAR and SARin data**

### 4.3.2 Surface Type Classification

The first step in the sea-ice freeboard retrieval is the surface type classification for each waveform based on pre-computed waveform shape parameters. The objective is assigning each waveform one of the four classification values:

1. Open ocean: Measurement over water surfaces outside the sea ice cover.
2. Lead: Measurement over water surfaces inside the sea ice cover between sea ice floes or at sea ice fractures.
3. Ice Surface: Measurements that solely consist of sea ice surfaces.
4. Ambiguous: Measurements from mixed surfaces or where the classification has failed

The surface type classification algorithm originates from algorithm development in the ESA Climate Change Initiative – Sea Ice Project (Paul et al., 2018) and classifies waveform based on three waveform parameters:

1. Pulse Peakiness (PP)
2. Leading Edge Width (LEW)
3. Radar backscatter coefficient (SIGMA0)

The pulse peakiness PP is computed based on the power of each range bin $WF_i$, the maximum power of the waveform $\max(WF)$ and the number of range bins $N_{wf}$ in the waveform:

$$PP = \sum_{i=1}^{N_{wf}} \frac{\max(WF)}{WF_i} \cdot N_{wf}$$

The leading-edge width LEW is computed using the TFMRA retracker algorithm (see section 4.3.3) for power thresholds of 5 and 95%.

The radar backscatter coefficient is computed after Dinardo, 2016.

The thresholds for the three parameters have independent values for SAR and SARin waveforms. In addition to the waveform-based classification, the sea-ice concentration data is providing the daily sea-ice mask and the land/sea flag (variable surf_type_01) from the L1b input data set is used to exclude any data over land. The land/sea flag is provided at 1Hz in the L1b files and its values is replicated to all 20Hz waveforms within the 1 second window.

After classification, the surface type flag is merged with the land/sea flag for further use in the processor into a single flag container that contains the external mask-based land/ocean information and the ice/water flag from the waveform-based classification.

#### 4.3.2.1 Open Ocean

Measurements over open ocean are classified solely by the sea-ice concentration auxiliary data set and the land/sea flag: Every waveform that is marked as ocean (variable surf_type_01 is 0) and where the sea ice concentration is below 70%. The threshold is higher than the usual value (15%) for the ice edge in sea-ice concentration data sets from passive microwave observations. The higher threshold is intended to prevent misclassifications of other surface types in loose ice conditions of the marginal ice zone and thus the open ocean domain intentionally includes potentially ice-covered region.

#### 4.3.2.2 Lead Surface

Radar altimeter measurements over leads within the sea ice cover are characterized by specular reflection, resulting in narrow echoes with a high peak power. To be classified as a lead waveform, PP and SIGMA0 must exceed a minimum threshold, while LEW must be smaller than a maximum threshold. The following parameter thresholds are valid for Arctic sea ice in the winter period between October and April:

**Table 5: Waveform shape parameter thresholds for lead surface classification of CryoSat-2 SAR waveforms in the Arctic**

| Arctic Leads (SAR) | SIC | PP | | LEW | | SIGMA0 | |
|---|---|---|---|---|---|---|---|
| | MIN | MIN | MAX | MIN | MAX | MIN | MAX |
| October | 70% | 67.30 | - | - | 0.77 | 23.80 | - |
| November | 70% | 66.30 | - | - | 0.78 | 23.20 | - |
| December | 70% | 66.60 | - | - | 0.78 | 23.30 | - |
| January | 70% | 69.90 | - | - | 0.76 | 23.40 | - |
| February | 70% | 76.00 | - | - | 0.72 | 28.00 | - |
| March | 70% | 73.80 | - | - | 0.73 | 25.80 | - |
| April | 70% | 68.60 | - | - | 0.76 | 24.10 | - |

**Table 6: Waveform shape parameter thresholds for lead surface classification of CryoSat-2 SARin waveforms in the Arctic**

| Arctic Leads (SARin) | SIC | PP | | LEW | | SIGMA0 | |
|---|---|---|---|---|---|---|---|
| | MIN | MIN | MAX | MIN | MAX | MIN | MAX |
| October | 70% | 264.30 | - | - | 1.10 | 24.90 | - |
| November | 70% | 257.90 | - | - | 1.11 | 25.00 | - |
| December | 70% | 253.60 | - | - | 1.13 | 24.10 | - |
| January | 70% | 264.60 | - | - | 1.09 | 24.50 | - |
| February | 70% | 291.80 | - | - | 1.02 | 29.00 | - |
| March | 70% | 288.80 | - | - | 1.03 | 27.40 | - |
| April | 70% | 272.60 | - | - | 1.07 | 25.80 | - |

### 4.3.2.3 Sea Ice Surfaces

Radar backscatter of potentially rough sea ice surfaces may still return narrow echoes with higher return power than open ocean waveforms, but are distinctively lower PP, SIGMA0 and higher LEW than lead waveforms. The following parameter thresholds are valid for Arctic sea ice in the winter period between October and April:

**Table 7: Waveform shape parameter thresholds for sea ice surface classification of CryoSat-2 SAR waveforms in the Arctic**

| Arctic Sea Ice (SAR) | SIC | PP | | LEW | | SIGMA0 | |
|---|---|---|---|---|---|---|---|
| | MIN | MIN | MAX | MIN | MAX | MIN | MAX |
| October | 70% | - | 30.50 | 1.02 | - | 2.5 | 20.80 |
| November | 70% | - | 28.70 | 1.08 | - | 2.5 | 19.90 |
| December | 70% | - | 28.10 | 1.10 | - | 2.5 | 19.60 |
| January | 70% | - | 28.50 | 1.11 | - | 2.5 | 19.00 |
| February | 70% | - | 35.40 | 0.91 | - | 2.5 | 25.70 |
| March | 70% | - | 34.90 | 0.90 | - | 2.5 | 23.20 |
| April | 70% | - | 31.90 | 0.97 | - | 2.5 | 21.10 |

**Table 8: Waveform shape parameter thresholds for sea ice surface classification of CryoSat-2 SARin waveforms in the Arctic**

| Arctic Sea Ice (SARin) | SIC | PP | | LEW | | SIGMA0 | |
|---|---|---|---|---|---|---|---|
| | MIN | MIN | MAX | MIN | MAX | MIN | MAX |
| October | 70% | - | 99.40 | 1.55 | - | 2.5 | 21.40 |
| November | 70% | - | 94.20 | 1.58 | - | 2.5 | 20.90 |
| December | 70% | - | 89.90 | 1.62 | - | 2.5 | 20.10 |
| January | 70% | - | 90.00 | 1.64 | - | 2.5 | 19.10 |
| February | 70% | - | 114.40 | 1.44 | - | 2.5 | 24.30 |
| March | 70% | - | 113.90 | 1.44 | - | 2.5 | 23.70 |
| April | 70% | - | 103.80 | 1.51 | - | 2.5 | 22.00 |

#### 4.3.2.4 Ambiguous Surfaces

All waveforms that are not classified as one of the other surface types or as land by the land/sea flag are designated as ambiguous and discarded from further processing.

### 4.3.3 Threshold First Maximum Retracker Algorithm (TFMRA)

A retracking algorithm determines the range from the spacecraft altimeter sensor to the dominant backscatter surface, as several backscatter sources may contribute to a single radar waveform. For lead and sea ice surfaces it is assumed that the range to the surface is located on the leading edge at the half-power point (power threshold) of the first significant maximum of the waveform.

The specific TFMRA implementation used in Cryo-TEMPO is oriented after the implementation used in Ricker et al., 2014. The algorithm only depends on the leading edge of the waveform before the first maximum. The algorithm to determine the range at the leading edge when the power level has crossed a certain threshold can be implemented in robust and numerical efficient way. But as also shown by Ricker et al., 2014, the results over sea ice are critically dependent on the power threshold values for both lead and sea ice waveforms. The thresholds for lead (50%) and sea ice surfaces (50%) used here originate from the ESA Climate Change Initiative sea ice project and have been chosen due to a better representation of the seasonal cycle of Arctic sea ice thickness then alternative fixed threshold parametrizations, e.g., by setting both power thresholds for water and ice surfaces to 80% (Khvorostovsky et al., 2020).

CryoSat-2 waveforms are sampled in discrete intervals at a resolution of 0.2342m for SAR and SARin radar modes that can be coarse for the narrow waveforms of lead respectively smooth and undeformed sea ice. The TFMRA implementation there uses a filtered representation of the sampled waveforms from the L1B data to counter the aliasing effect. The filtering parametrization differs for SAR and SARin waveforms to account for the different noise level of the two radar modes.

Specifically, the following processing steps are executed by the TFMRA implementation:

1. Waveform oversampling by a factor of 10 using linear interpolation of the L1B waveform power.
2. Smoothing of the oversampled waveform using a box filter with the width of 11 points for SAR waveform and 21 points for SARin waveforms. The reason for a larger smoothing of SARin waveforms is higher noise levels.
3. Normalizing of the filtered waveform power (maximum power has the value of 1.0)
4. Detection of the first maximum on the filtered and normed waveform power as the first point that exceeds the value of 0.15 for SAR and 0.45 for SARin waveforms
5. Estimation of the position within the range window with a rise to 50% of the power of the first maximum by linear interpolation between the two closest points of the filtered waveform.

6. TFMRA retracker range is then computed by adding position within the range window to the window delay corrected for center of mass and other corrections (variable window_del_20_ku in the L1B file).

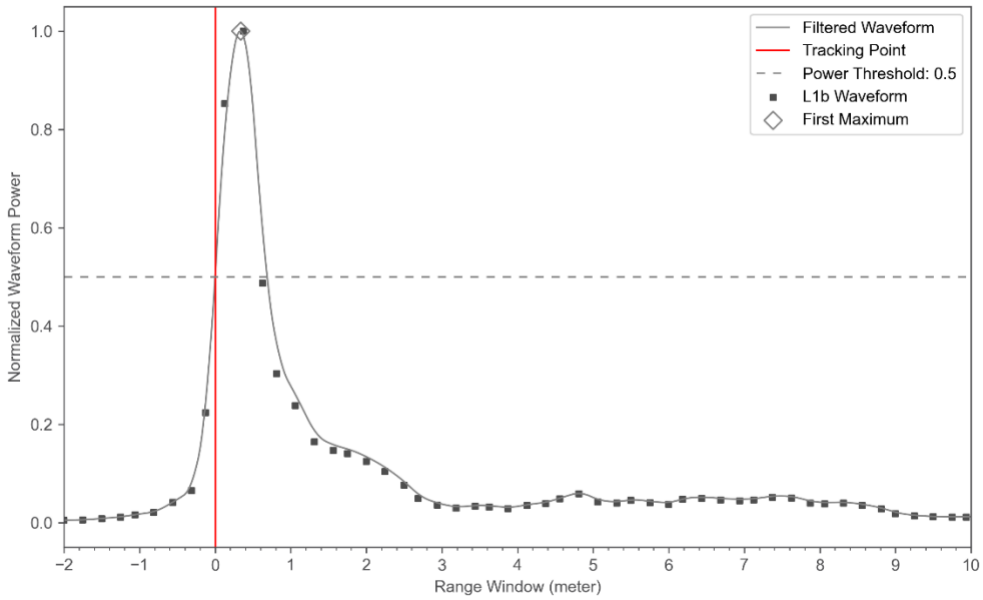


**Figure 8: Schematic of the TFMRA implementation. The retracking point is estimated when the filtered waveform exceeds a power threshold at the leading edge.**

| TFMRA Algorithm Parameter | Value |
|---|---|
| Waveform Oversampling Factor | 10 |
| Smoothing box filter size (oversampled range bins) | 11 SAR / 21 SARin |
| First Maximum normalized power threshold | 15% SAR / 45% SARin |
| Retracker power threshold | 50% (for all surface types and radar modes) |

Each waveform identified as either lead or sea ice by the surface type classification is retracked by TFMRA with a 50% power threshold. The retracker returns the location of the surface within the range window of the full waveform. This information is then used to compute the range $r$ from the center of mass of the spacecraft to the surface by adding the window delay (variable window_del_20_ku). The window delay refers to the two-way time of the transmitted and received radar pulse with respect to the center of the waveform range windows and is already corrected for instrument delays. The two-way time is converted into range using the speed of light in vacuum.

The TFMRA algorithm does not provide an uncertainty value, therefore it is parametrized with 0.1m. This value has been empirically derived by evaluating the standard deviation over larger stretches of thin and presumable flat sea ice.

### 4.3.4 Surface Elevations and Range Corrections

The TFMRA range $r$ and the altitude of the center of gravity of the spacecraft $h_{cog}$ provide information of the surface elevation $h_{surface}$ with respect to the reference ellipsoid. At this stage, the range has been computed based on the speed of light in vacuum and corrections need to be applied for varying wave propagation speed depending on the condition of the troposphere and ionosphere. In addition, tidal corrections are applied to range for consistency of elevations of ocean surfaces for different data acquisitions:

$$h_{surface} = h_{cog} - r + \sum r_c$$

The list of range corrections $r_c$ is the following:

- Ionosphere correction (source: L1b)
- Dry troposphere correction (source: L1b)
- Wet troposphere correction (source: L1b)
- Dynamic atmosphere correction (source: L1b)
- Elastic ocean tide (source: RegAT-Arctic)
- Long-period ocean tide (source: RegAT-Arctic)
- Ocean loading tide (source: RegAT-Arctic)
- Solid earth tide (source: L1b)
- Geocentric polar tide (source: L1b)

There are two data sources for the different range correction: Corrections for range effects caused by conditions in the ionosphere, troposphere as well as the dynamic atmosphere correction, which combines the inverse barometric effect with the high-frequency fluctuations of the ocean surface. These parameters and the solid earth tide and polar tide are based on information present in the Level-1b primary input data (see section 4.1.1). The remaining tidal corrections are sourced from the more recent and RegAT-Arctic regional model (Cancet et al., 2022, in prep.).

### 4.3.5 Sea Surface Anomaly and Radar Freeboard

After application of the range correction, the surface heights split into two categories, the heights of lead surfaces and the heights of sea ice surfaces.

The heights of the lead surfaces with respect to the mean sea surface ($mss$) yield raw observations of the sea level anomaly ($sla_{raw}$) at discrete locations where the surface type classification indicates the presence of a lead:

$$sla_{raw} = h_{surface}[surface\ type \equiv lead] - mss$$

The discrete sea-level anomaly observations must be extended to all ice surfaces as reference for the ice surface heights. This is achieved by an interpolating and smoothing function that provides a continuous sea level anomaly ($sla$):

$$sla = func(sla_{raw})$$

The function contains several main processing steps:

1. Smooth $sla_{raw}$ with a box filter with filter size of 100km to reduce the raw noise of the observations. This step is only applied to the existing observations. The filter size width has been chosen empirically as a compromise in reducing noise and retaining true spatial variability of the sea surface height.
2. Apply a linear interpolation between the smoothed raw sea-level anomaly observations for the entire trajectory.
3. Apply a box-filter smoother to the interpolated values with the same filter size as before (100 km).
4. Set the result to NaN (not a number) if the closest $sla_{raw}$ observation is not within two times the filter size (200km).

The output is a smoothed and interpolated sea-level anomaly ($sla$) that extends along the entire ice-covered area if enough leads are present.

The uncertainty of this approach is parametrized with the following formular and based on the distance$d_{tp}$ to the next $sla_{raw}$ tie point. The uncertainty increases with distance to raw sea-level anomaly observations and reaches its maximum at 100km. The uncertainty reaches its minimum at the location of a raw sea-level anomaly observation, and it is assumed that the smoothing process results in an uncertainty of 0.02 m:

$$\sigma_{sla} = \begin{cases} 0.02m + 0.1m \times \left({}^{d_{tp}}/_{100km}\right)^2, & d_{tp} < 100km \\ 0.1m, & d_{tp} \geq 100\ km \end{cases}$$

Subtracting the sum of sea level anomaly and mean sea surface from the sea ice heights $h_{ice}$ then yield radar freeboard $f_{radar}$. The parameter is defined as the freeboard as measured directly by the radar altimeter from range differences of ice surfaces and the local sea level without further corrections or use of auxiliary data sets.

$$\begin{aligned} h_{ice} &= h_{surface}[surface\ type \equiv sea\ ice] \\ f_{radar} &= h_{ice} - (mss + sla) \\ &= h_{ice} - ssh \end{aligned}$$

The radar freeboard uncertainty is then defined as:

$$\sigma_{fradar} = \sqrt{\sigma_{hice}{}^2 + \sigma_{sla}{}^2}$$

With the assumption that the mean sea surface uncertainty is included in the sea level anomaly uncertainty.

### 4.3.6 Sea Ice Freeboard

Radar freeboard differs from sea-ice freeboard by a range correction that takes the slower wave propagation speed in the snow layer into account. Without this correction and in the presence of a significant snow layer, the radar freeboard underestimates the true sea-ice freeboard $f_{ice}$:

$$f_{ice} = f_{radar} + \Delta r_{snow}$$

The range correction depends both on the snow depth $sd$ that controls the affected fraction of the travel path as well as the snow density $\rho_s$, which controls the wave propagation speed in the snow layer $c_s$ that differs from vacuum lightspeed $c$:

$$\Delta r_{snow} = \left(\frac{c}{c_s} - 1\right) \cdot sd$$

$$c_s = c\ (1 + 0.51\ \times \rho_s)^{-1.5}$$

The density of snow on sea ice is increasing throughout the winter season and it is parametrized as a function of time $t$ that is represented the elapsed fractional month since October 15:

$$\rho_s = 6.5\ \times \mathrm{t} + 274.51$$

The source for the computation of the $\Delta r_{snow}$ is Mallet et al., 2020. There is no uncertainty information for the snow density parametrization, so the sea-ice freeboard uncertainty is computed based on the uncertainties of the radar freeboard and snow depth:

$$\sigma_{fice} = \sqrt{\sigma_{fradar}{}^2 + \left(\frac{c}{c_s} - 1\right)^2 \cdot \sigma_{sd}{}^2}$$

### 4.3.7 Filtering

As a final step in the processing, sea-ice freeboard values outside the range of -0.25 to 2.25 meter are removed and set to not-a-number (NaN) to exclude unrealistic observations due to a misclassification or surface targets that are not sea ice, e.g., icebergs. The NaN mask of the sea-ice freeboard is then also applied to radar freeboard, to keep the two variables consistent.

# 5 EXAMPLES

## 5.1 Trajectory Sea-Ice Freeboard

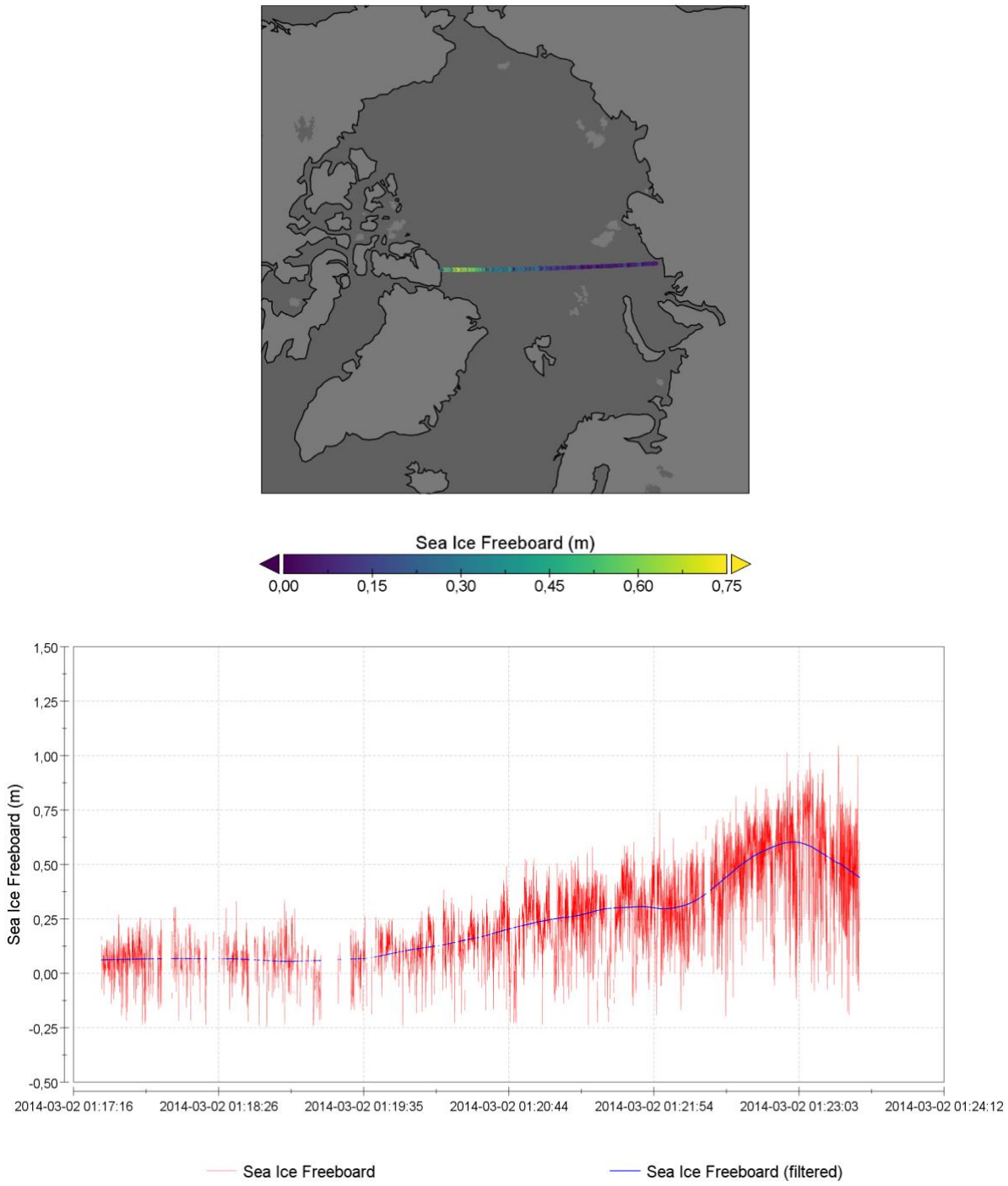


**Figure 9: Sea-ice freeboard example from absolute orbit number 20658 on March 2, 2014. Upper panel: Map, lower panel: Along-track (east to west on map) of sea-ice freeboard and filtered sea ice freeboard.**

# 6 KNOWN ISSUES

There are several known limitations and error contributions in the sea-ice freeboard retrieval process with radar altimeter data that affects the uncertainty of the variables in the Cryo-TEMPO thematic sea ice product. Most prominently is the large variability of the sea ice surface and its snow cover throughout the stages of development of sea ice that can strongly influence the return signal of a radar altimeter. The most prominent potential error contributions for sea-ice freeboard from CryoSat-2 radar altimeter data that must be noted are:

1. Snow depth on sea ice has a direct impact on the sea-ice freeboard process, but observations are not available for the full CryoSat-2 data record. Climatological data is used in the absence of direct observations and consequently, the regional, seasonal and interannual variability and change of snow depth is not fully captured. A fraction of approximately 20% of the snow depth error propagates into the sea-ice freeboard error.
2. The sea-ice freeboard retrieval assumes that radar backscatter from the snow layer has a negligible effect on the waveform shape and that the impact of snow is limited to a signal delay due to lower the radar wave propagation speed than in vacuum. Several studies however have demonstrated (Kwok 2014; Kurtz et al., 2014; Ricker et al., 2015; Nandan et al., 2017) that snow interface and volume backscatter influence retracker range under certain physical conditions. However, including this effect into the sea-ice freeboard retrieval requires the information on the properties of the snow layer, which are currently unavailable at basin scale. As a result, sea-ice freeboard may be biased high in the order of a few centimetres in periods and regions where backscatter from the snow layer is relevant.
3. The shape of the radar waveform and thus the tracking point at the leading edge of the waveform also depends on the roughness and backscatter properties of the surface. Empirical retrackers with fixed power thresholds as used in the current version of the Cryo-TEMPO thematic sea ice product are likely to overestimate the freeboard for sea ice surfaces with high surface roughness (Landy et al., 2020). Strategies to mitigate this issue are under development and scheduled for future evolutions of the thematic sea ice product, including the use of physical waveform models that take a variable surface roughness into account. It also must be noted that rough surfaces are able to trap more snow and that the issues of snow backscatter and impact of surface roughness are likely correlated, with both resulting in a positive freeboard bias.
4. Version 2 of the C3S / OSI-SAF sea ice type climate data record used for sea ice classification (see section 4.1.2.2) contains only the ambiguous class in the first 15 days of each October. From October 16 on, the full classification of first-year ice, multi-year ice and ambiguous is available. This causes a discontinuity in the ice type-based correction of the snow climatology.

# 7 REFERENCES

Cancet, M., Lyard F., Toublanc F., Pineau-Guillou L., Sahuc E., Fouchet E., Dibarboure G., Picot N., The RegAt high-resolution regional tidal model in the North-East Atlantic Ocean: implementation and examples of applications, in preparation (2022)

Dinardo, S. (2016): Guidelines for reverting Waveform Power to Sigma Nought for CryoSat-2 in SAR mode. Issue 2, Revision 2, ESA document ref: XCRY-GSEG-EOPS-TN-14-0012,

Khvorostovsky, K.; Hendricks, S.; Rinne, E. Surface Properties Linked to Retrieval Uncertainty of Satellite Sea-Ice Thickness with Upward-Looking Sonar Measurements. Remote Sens. 2020, 12, 3094. https://doi.org/10.3390/rs12183094

Kurtz, N. T., Galin, N., and Studinger, M.: An improved CryoSat-2 sea ice freeboard retrieval algorithm through the use of waveform fitting, The Cryosphere, 8, 1217–1237, https://doi.org/10.5194/tc-8-1217-2014, 2014.

Kwok, R. (2014), Simulated effects of a snow layer on retrieval of CryoSat-2 sea ice freeboard, *Geophys. Res. Lett.*, 41, 5014– 5020, doi:10.1002/2014GL060993.

Mallett, R. D. C., Lawrence, I. R., Stroeve, J. C., Landy, J. C., and Tsamados, M.: Brief communication: Conventional assumptions involving the speed of radar waves in snow introduce systematic underestimates to sea ice thickness and seasonal growth rate estimates, The Cryosphere, 14, 251–260, https://doi.org/10.5194/tc-14-251-2020, 2020.

Markus, T. and Cavalieri, D.J. (1998). Snow Depth Distribution Over Sea Ice in the Southern Ocean from Satellite Passive Microwave Data. In Antarctic Sea Ice: Physical Processes, Interactions and Variability, M.O. Jeffries (Ed.). https://doi.org/10.1029/AR074p0019

Nandan, V., Geldsetzer, T., Yackel, J., Mahmud, M., Scharien, R., Howell, S., … Else, B. (2017). Effect of snow salinity on CryoSat-2 Arctic first-year sea ice freeboard measurements. *Geophysical Research Letters*, 44, 10,419– 10,426. https://doi.org/10.1002/2017GL074506

Landy, J. C., Petty, A. A., Tsamados, M., & Stroeve, J. C. (2020). Sea ice roughness overlooked as a key source of uncertainty in CryoSat-2 ice freeboard retrievals. Journal of Geophysical Research: Oceans, 125, e2019JC015820. https://doi.org/10.1029/2019JC015820

Lavergne, T., Kern, S., Aaboe, S., Derby, L., Dybkjaer, G., Garric, G., Heil, P., Hendricks, S., Holfort, J., Howell, S., Key, J., Lieser, J. L., Maksym, T., Maslowski, W., Meier, W., Muñoz-Sabater, J., Nicolas, J., Özsoy, B., Rabe, B., Rack, W., Raphael, M., de Rosnay, P., Smolyanitsky, V., Tietsche, S., Ukita, J., Vichi, M., Wagner, P., Willmes, S., & Zhao, X. (2022). A New Structure for the Sea Ice Essential Climate Variables of the Global Climate Observing System, Bulletin of the American Meteorological Society, 103(6), E1502-E1521.

Paul, S., Hendricks, S., Ricker, R., Kern, S., and Rinne, E.: Empirical parametrization of Envisat freeboard retrieval of Arctic and Antarctic sea ice based on CryoSat-2: progress in the ESA Climate Change Initiative, The Cryosphere, 12, 2437–2460, https://doi.org/10.5194/tc-12-2437-2018, 2018.

Ricker, R., Hendricks, S., Helm, V., Skourup, H., and Davidson, M.: Sensitivity of CryoSat-2 Arctic sea-ice freeboard and thickness on radar-waveform interpretation, The Cryosphere, 8, 1607–1622, https://doi.org/10.5194/tc-8-1607-2014, 2014.

Ricker, R. , Hendricks, S. , Perovich, D. K. , Helm, V. and Gerdes, R. (2015): Impact of snow accumulation on CryoSat-2 range retrievals over Arctic sea ice: An observational approach with buoy data , Geophysical Research Letters, 42 (11), pp. 4447-4455 . doi: 10.1002/2015GL064081

Rostosky, P., Spreen, G., Farrell, S. L., Frost, T., Heygster, G., & Melsheimer, C. (2018). Snow depth retrieval on Arctic sea ice from passive microwave radiometers—Improvements and extensions to multiyear ice using lower frequencies. Journal of Geophysical Research: Oceans, 123, 7120– 7138. https://doi.org/10.1029/2018JC014028

Warren, S. G., Rigor, I. G., Untersteiner, N., Radionov, V. F., Bryazgin, N. N., Aleksandrov, Y. I., & Colony, R. (1999). Snow Depth on Arctic Sea Ice, Journal of Climate, 12(6), 1814-1829. Retrieved Feb 17, 2021, from https://journals.ametsoc.org/view/journals/clim/12/6/1520-0442_1999_012_1814_sdoasi_2.0.co_2.xml